# Single-Molecule Force Spectroscopy of Rapidly Fluctuating, Marginally Stable Structures in the Intrinsically Disordered Protein $\alpha$-Synuclein

Allison Solanki,[1] Krishna Neupane,[1] and Michael T. Woodside[1,2]
[1]Department of Physics, University of Alberta, Edmonton, Alberta T6G 2E1, Canada
[2]National Institute for Nanotechnology, National Research Council Canada, Edmonton, Alberta T6G 2M9, Canada
(Received 29 November 2013; revised manuscript received 5 March 2014; published 16 April 2014)

Intrinsically disordered proteins form transient, fluctuating structures that are difficult to observe directly. We used optical tweezers to apply force to single $\alpha$-synuclein molecules and measure their extension, characterizing the resulting conformational transitions. Force-extension curves revealed rapid fluctuations at low force, arising from the folding of two different classes of structure that were only marginally stable. The energy landscape for these transitions was characterized via the force-dependent kinetics derived from correlation analysis of the extension trajectories. The barriers were small, only a few $k_BT$, but the diffusion was slow, revealing a landscape that is flat but rough.

DOI: 10.1103/PhysRevLett.112.158103 PACS numbers: 87.15.Cc, 87.15.hp, 87.80.Cc, 87.80.Nj

Most proteins form well-defined, thermodynamically stable structures. Because of the deep connection between structure and function, the elucidation of structures from a wide range of proteins represents one of the signature achievements of biophysical science. It has become clear, however, that a significant number of proteins lack any stable structure, being instead intrinsically disordered [1,2]. Such disorder may allow a single protein to play diverse roles [3,4] by forming distinct structures with different functions triggered by specific conditions (e.g., ligand binding); it may also provide other advantages, such as increasing the rate of molecular association owing to a greater capture radius than for folded proteins [5]. Indeed, intrinsically disordered proteins (IDPs) carry out a wide range of important functions, from cell-cycle control to transcriptional and translational regulation [6]. On the other hand, conformational disorder also seems to heighten a protein's susceptibility to misfolding and aggregation, and many IDPs are involved in aggregation-related diseases, including $A\beta$ and tau (linked to Alzheimer's disease) as well as $\alpha$-synuclein (linked to Parkinson's disease) [7].

Traditional approaches to structure-function studies have limited utility for IDPs. Structures formed in the presence of ligands or other stabilizing conditions (e.g., membrane or micelle binding, protein-protein interactions) can sometimes be solved by traditional ensemble methods [8,9], but the transient structures formed under disordered conditions are difficult to discern. Novel probes of structure and dynamics in IDPs are thus of great interest. Single-molecule (SM) approaches offer powerful advantages for characterizing the conformations of IDPs, since they can monitor the dynamic, transient structures formed by disordered proteins. Notably, SM Förster resonant energy transfer—in which resonant energy transfer between dye molecules is used to monitor changes in the structure—has been applied to observe conformational fluctuations in IDPs such as $\alpha$-synuclein [9–12]. These studies have identified the presence of partially folded intermediates and probed their modulation by conditions such as different solution environments (including the presence of surfactants [9–11] or changes in $p$H [12]).

Here we describe an alternate approach, using SM force spectroscopy—in which the end-to-end molecular extension is measured as the conformation changes in response to an applied force—to characterize structural fluctuations in single molecules of human $\alpha$-synuclein. Found primarily at presynaptic terminals in the brain, $\alpha$-synuclein is an intrinsically disordered protein *in vitro* [13], but interacts with lipids to form various helical structures [14,15], and can aggregate into $\beta$-sheeted amyloid fibrils [16]. Force spectroscopy studies using atomic force microscopes (AFMs) found that $\alpha$-synuclein can sometimes form various mechanically stable structures in monomers [17,18] and dimers [19]. However, the stiff force probes used in these measurements lacked the force resolution needed to observe structures having only marginal stability —the kind of structures that would be expected to be prevalent among the conformational fluctuations of IDPs. Optical tweezers, which have much lower stiffness and hence higher force resolution [20], are more suitable for probing such structures. Optical tweezers have been used to study transient mechanically stable structures formed by $\alpha$-synuclein [21], but they have not yet been applied to characterize low-energy fluctuations in IDPs.

To probe structural fluctuations in $\alpha$-synuclein, single protein molecules were attached covalently to double-stranded DNA handles as described previously [22]. The handles were attached in turn to micron-sized polystyrene beads held in a dual-beam, high-resolution optical trap [Fig. 1(a), inset] [23]. The protein constructs consisted of either a single $\alpha$-synuclein monomer, or tandem repeats (both dimeric and tetrameric) of $\alpha$-synuclein linked end-to-

 

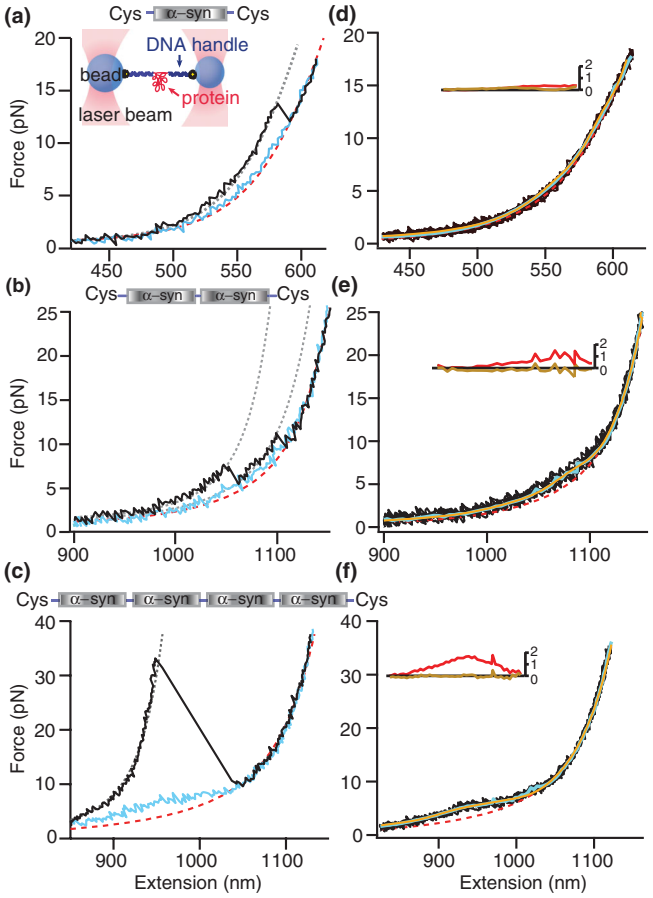


FIG. 1 (color). Force spectroscopy of $\alpha$-synuclein. (a) Inset: A single protein molecule was attached at its ends to DNA handles, bound to beads and held under tension between two optical traps. FECs of $\alpha$-synuclein monomers sometimes revealed discrete unfolding rips (black), but usually showed a monotonic rise in force with extension without obvious rips (cyan). Similar behavior was seen for $\alpha$-synuclein dimers (b) and tetramers (c). FECs without rips nevertheless deviated from WLC behavior (red). (d)–(f) FECs without discrete rips were averaged (cyan) and compared to polymer models. Data did not fit a noninteracting WLC model (red; residuals in inset), but did fit a model incorporating rapid structural fluctuations, Eq. (1) (yellow; residuals in inset).

end (Fig. S1 of the Supplemental Material [24]), similar to those used in other force spectroscopy assays [31] and prepared as described previously [21]. The force applied to the molecule was ramped up and down by moving the traps apart or together at a constant speed [24]; plotting force against molecular extension generated a series of force-extension curves (FECs).

FECs occasionally displayed discrete "rips," in which the extension increased abruptly concomitant with a sudden decrease in the force [Figs. 1(a)–(c), black]. Such behavior, characteristic of the cooperative unfolding of mechanically stable structures, is qualitatively similar to that observed previously in AFM measurements [17–19]. It reflects the formation, via transient conformational fluctuations, of metastable structures with sufficiently large energy barriers to withstand high unfolding forces during rapid force ramps, as shown previously [21]. These FECs were well fit on each side of the rip by a polymer elasticity model consisting of two extensible wormlike chains (WLCs) in series [Eq. (S1) [24]], one for the DNA handles and the other for the unfolded protein [21,22]. Here, we are interested instead in the majority of FECs that showed no discrete rips, but rather a monotonic rise in force with extension [Figs. 1(a)–1(c), cyan].

Interestingly, the FECs without discrete unfolding rips did not fit well to a simple WLC model, as would be expected for a noninteracting (unfolded) polymer. Averaging the FECs for each set of curves measured on a single molecule to reduce the noise [Figs. 1(d)–1(f), cyan], fits to the WLC expected for the fully unfolded protein (Fig. 1, dashed red line) yielded residuals with systematic deviations from zero [Figs. 1(d)–1(f) inset, red]. The residuals were largest for the tetrameric construct [Fig. 1(f)] and smallest for the monomer [Fig 1(d)], but in all cases nonrandom (see Supplemental Material [24]), indicating an incomplete fit. The deviation from pure WLC behavior produced a "shoulder" feature in the force range ~2–8 pN. Such deviations are not typically present in FECs of unfolded proteins [22,32,33], nor were they observed in control measurements of the DNA handles alone (Fig. S2 [24]), indicating that they are a property specifically of $\alpha$-synuclein. Because the extension at a given force within the shoulder feature is lower than would be expected in a WLC, attractive interactions must be forming as the force is lowered, making the protein more compact than expected, even though no cooperative unfolding transitions could be discerned directly. The same characteristic shape was observed for refolding FECs as for unfolding FECs (Fig. S3, black), indicating reversible (i.e., equilibrium) behavior.

Motivated by qualitatively similar shoulderlike features seen in FECs of the ultrafast folding protein villin [34] and of mRNA transcripts that could form an ensemble of small, fast-folding hairpins [35], we interpreted the shoulder features in terms of rapid, quasiequilibrium unfolding or refolding of structures that are only marginally stable. In this picture, the fact that deviations from WLC behavior occur only at low force results from the marginal stability of the structures. In turn, the reversibility of the FECs and apparent lack of cooperativity both result from the fast kinetics. In particular, whereas the sharp, sawtoothlike rip patterns commonly seen in force spectroscopy measurements arise from folding and unfolding rates that are slow compared to the FEC step dwell time (1–5 ms), rates that are fast compared to the dwell times result in a quasiequilibrium average over multiple transitions. Such averaging will produce a FEC that appears to move smoothly, as the force is increased, between the WLC curve expected for the

TABLE I. Fits of the FEC shoulder features to Eq. (1). Fit parameters are the same for both dimer and tetramer, but there are twice as many transitions in the latter. Uncertainties represent standard errors.

| Sample | $N^1$ | $\Delta L_c^1$ (nm) | $F_{1/2}^1$ (pN) | $\Delta G^1$ ($k_BT$) | $N^2$ | $\Delta L_c^2$ (nm) | $F_{1/2}^2$ (pN) | $\Delta G^2$ ($k_BT$) |
|---|---|---|---|---|---|---|---|---|
| Dimer | $4 \pm 1$ | $14 \pm 2$ | $3.6 \pm 0.4$ | $1.5 \pm 0.4$ | $3 \pm 1$ | $9 \pm 1$ | $6.5 \pm 0.7$ | $2.4 \pm 0.5$ |
| Tetramer | $9 \pm 1$ | $15 \pm 2$ | $3.9 \pm 0.4$ | $1.8 \pm 0.5$ | $8 \pm 1$ | $8 \pm 1$ | $7.2 \pm 0.5$ | $2.7 \pm 0.6$ |

folded state and that expected for the unfolded state, without any detectable rips [34]. In this case, the shoulder in the FEC will have a shape defined by the force-dependent probability that the structure is unfolded, $P_u(F)$.

To test this picture quantitatively, we constructed a minimal model for the protein, assuming that it can form some number of independent structures via two-state transitions in rapid equilibrium [24]. The extension as a function of force was then taken as the sum of the extension of the handle, $x_H(F)$ [obtained by inverting Eq. (S1) [24] for the DNA], the extension of the fully unfolded part of the polypeptide chain $x_{PU}(F)$, and the sum of the extensions of the various protein structures that are unfolding concurrently in rapid equilibrium,

$$x(F) = x_H(F) + x_{PU}(F) + \sum_{i=1}^{n} N_i[P_u^i(F)\Delta x_i(F)]. \quad (1)$$

Here, $n$ is the number of different types of transitions having distinct unfolding properties (each assumed to act as a two-state system). The model allows for the possibility that several structures might share similar unfolding properties, with the parameter $N_i$ denoting the number of instances of each type of transition (note that this means the model cannot distinguish between distinct structures that have similar unfolding properties). If the structures involve only intra-monomer interactions, $N_i$ should scale as the number of monomers in the protein construct. For two-state unfolding in equilibrium, $P_u(F) = [1 + \exp\{\beta(F_{1/2} - F)\Delta x(F)\}]^{-1}$, where $F_{1/2}$ is the force at which the structure has 50% probability of being unfolded and $\Delta x(F)$ is the extension change upon unfolding at force $F$ [from which the contour length change upon unfolding $\Delta L_c$ can be found by inverting Eq. (S1) [24] ] [36]. Each type of transition in the model is thus characterized by unique $F_{1/2}$ and $\Delta L_c$ values.

To determine the variant of the model that best explained the observed shoulder features, the FECs for each molecule were averaged [as in Figs. 1(d)–1(f), cyan] and fit to Eq. (1), then a series of statistical tests were used to judge whether the model variant was adequate to fit the data [24]. Multiple model variants were tested in this way [24]; the simplest one able to fit all the data had $n = 2$ and $N_i > 1$, indicating the presence of two different types of transitions with distinct $F_{1/2}$ and $\Delta L_c$ values, each consisting of an ensemble of structures having similar unfolding properties [Figs. 1(d)–1(f), yellow; Fig. S4 [24] ]. Independent fits to the tetramer and dimer FECs yielded the same results for the properties of the two classes of transitions: one class had $\Delta L_c \sim 15$ nm and $F_{1/2} \sim 3$–$4$ pN (denoted type 1), the other, $\Delta L_c \sim 8$ nm and $F_{1/2} \sim 7$ pN (denoted type 2). $N_1$ and $N_2$ were twice as large for the tetramer as for the dimer, as would be expected from the scaling of the protein lengths, with the fit values indicating two transitions of each type per monomer. The shoulder feature for the monomer was often too small to provide a reliable fit; however, the data were fully consistent with the model obtained from the fits to the dimers and tetramers (Fig. S5 [24]). We note that more complex model variants with additional fitting parameters showed evidence of overfitting [24], confirming that we found the minimal model for fitting the data. The fit results are listed in Table I.

To confirm that the shoulder features involved rapid structural transitions, as assumed in the model, we measured FECs for the tetramer without averaging the data at each step and investigated the kinetics of the extension fluctuations at different points in the curves. We then calculated the autocorrelation of the extension trajectories at different values of the average force (Fig. 2, triangles) [24]. For reference, we repeated these calculations for FECs measured using DNA handles alone, without any protein present (Fig. 2, circles). At all force values, the autocorrelation of the DNA handle extension showed a single-

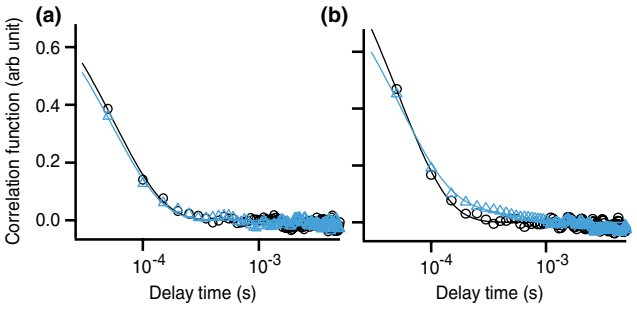


FIG. 2 (color online). Autocorrelation analysis of $\alpha$-synuclein tetramer. (a) The extension autocorrelation of a tetramer construct in the high-force range (>8 pN, triangles) demonstrates a single-exponential decay, and is identical to the result for a construct containing DNA handles only, without protein (circles). (b) In the midforce range (2–8 pN), where the shoulder feature is present in FEC data, the extension autocorrelation exhibits a single-exponential decay for the handle only (circles), but a double-exponential decay for the protein construct (triangles), indicating the presence of an additional mode corresponding to structural transitions in the protein.

exponential decay, with a time constant $\tau$ near 50 $\mu$s as expected for the handle and bead dynamics, which determine the time resolution of our trap [23,37]. At forces well above the $F_{1/2}$ fitting values, where no structural transitions should occur, the autocorrelation for handles plus protein was indeed indistinguishable from that for handles alone [Fig. 2(a)]. In the range 2–8 pN, however, the autocorrelation for the extension of the handles plus protein revealed an additional component in the exponential decay, which had a force-dependent time constant [Fig. 2(b), triangles]. This additional time constant was on the order of ~200–600 $\mu$s, slower than the time resolution of the instrument but faster than the step dwell time, consistent with the model described above.

The correlation time constant arising from a structural transition, $\tau$, can be related to the microscopic rates for folding ($k_f$) and unfolding ($k_u$) by $\tau(F) = [k_f(F) + k_u(F)]^{-1}$, where the microscopic rates are in turn related to the occupancies of the unfolded ($P_u$) and folded ($P_f$) states by $P_f/P_u = k_f/k_u$. We calculated $P_u$ and $P_f$ from the FEC fits (Table I), finding that type 1 transitions dominated the occupancies in the range 1–4 pN (Fig. S6, gray [24]), whereas type 2 transitions dominated in the range 6–8 pN (Fig. S6, black [24]). The microscopic rates for the transitions were then found from $\tau(F)$ as above, using the appropriate force ranges for type 1 [Fig. 3(a)] and type 2 [Fig. 3(b)] transitions. Notably, the force dependence of the rates was well fit in each case by the landscape model of Dudko *et al.* [38], which describes transition kinetics in terms of the underlying energy landscape governing the conformational dynamics. Fitting the microscopic rates to Eq. (S3) [Figs. 3(a),(b), solid lines], we found the distance to the energy barrier for the transition, $\Delta x^{\ddagger}$, the barrier height, $\Delta G^{\ddagger}$, and the transition rate at zero force, $k_0$ (Table SI [24]). As a check on the fit results, we compared the free-energy changes found from the FEC fitting for each type of transition to the values implied by the ratio of the folding and unfolding rates at zero force, as well as to the differences between the barrier heights for folding and unfolding found from the landscape analysis. In each case, good agreement was found (Table SII [24]), indicating that all the kinetic and equilibrium fits are consistent with one another. We also validated the assumption that each of the transitions is two state, by showing that the sum of the distances to the barrier from the folded and unfolded states is equal in each case to the total extension change upon unfolding found from the FEC fits (Table SII [24]).

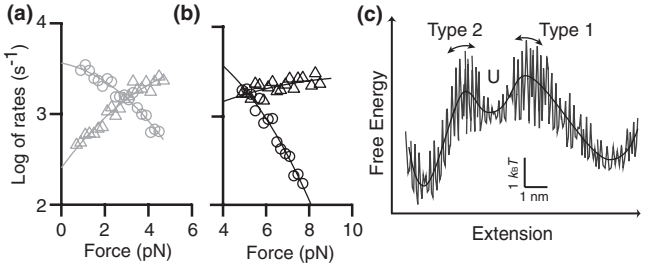


FIG. 3 Microscopic rates and energy landscape schematic. (a), (b) The microscopic rates for tetramer unfolding (triangles) and refolding (circles) of type 1 (gray) and type 2 (black) transitions are well fit by Eq. (S3) [24], yielding parameters describing the energy landscape. (c) Schematic of the energy landscape at zero force, showing the barriers, roughness, and free-energy changes for the two transitions.

What might these transitions represent structurally? Although $\alpha$-synuclein is largely disordered, structural and computational studies have found that it forms a condensed state, with long-range interactions between the negatively charged *C*-terminal region and both the negatively charged *N*-terminal region and the hydrophobic central NAC region, which have been postulated to inhibit aggregation in the native state [39,40]. Evidence was also found for interactions between the two halves of the *N*-terminal region, and a hydrophobic cluster at the *C* terminus [39,40]. Although we cannot directly identify the structures that form in our measurements, our observations are certainly consistent with the picture of a collapsed, molten-globule-like state held together by long-range contacts. From the $\Delta L_c$ values for the transitions, roughly 120 residues are sequestered within each monomer by the marginally stable structures, similar to the distance between the longest-range contacts found previously [39,40], and the low unfolding forces are what would be expected from weak long-range interactions [39–41]. Further support for this picture arises from the landscape analysis, which shows that the structures are mechanically compliant, having barriers that are located closer to the unfolded state than the folded state (Table SI [24]) and hence quite sensitive to force. Such compliant transitions are a hallmark of molten-globule states, owing to the lack of tertiary contacts imparting mechanical rigidity [42].

Considering the energy landscape for $\alpha$-synuclein in more detail, we note that, to our knowledge, the landscape profile for conformational fluctuations in an IDP has never before been quantified. The structures formed here are only marginally more stable than the unfolded state, by 2–3$k_BT$, in contrast to typical stabilities of ~10–20 $k_BT$ for natively structured proteins [23,31]. The barriers are also very low, only ~3–5 $k_BT$ for unfolding and ~0.5–1 $k_BT$ for folding, accounting for the rapidity of the fluctuations. By investigating the coefficient for conformational diffusion over the barrier, $D$, we also found that the landscape is quite rough. $D$ is the key parameter setting the time scale for microscopic motions of the protein (via the prefactor in Kramers' theory [43]). It can be deduced from the rates at zero force and the parameters describing the landscape profile [23,37],

$$D = \frac{\pi}{3}[k(\Delta x^{\ddagger})^2/\beta\Delta G^{\ddagger}]\exp(\beta\Delta G^{\ddagger}). \quad (2)$$

$D$ was calculated both for folding and unfolding, for each of the two transition types; in each case, the values found for

folding and unfolding agreed. Similar values of $D$ were found for both transition types, $D \sim 5 \times 10^{-14\pm0.7}$ m$^2$/s. This result is slower than the intrachain diffusion found for $\alpha$-synuclein from the chain reconfiguration time in fluorescence-quenching measurements, $\sim 10^{-11}$ m$^2$/s [44], as well as the diffusion coefficient found similarly in many other unfolded proteins and peptides [45–47]. It is also slower than $D$ for crossing the native folding barrier in the protein PrP, $1 \times 10^{-12\pm0.4}$ m$^2$/s [23], one of the few other measurements of $D$ across a barrier. Assuming that the slower diffusion we observe arises primarily from roughness in the landscape at the barriers for formation of the marginally stable structures, a random roughness distribution would imply fluctuations in the landscape of $\sim$2–3 $k_BT$ [48]. Such a roughness is quite large, comparable to the largest values reported for natively structured proteins [49]. It is also similar to the energy differences between the states as well as the height of the barriers. The picture that emerges is thus one of a landscape that is quite flat but rugged [Fig. 3 (c)], in contrast to the strongly funneled shape typical of landscapes for natively structured proteins [50,51], directly confirming the qualitative landscape model that has been generally assumed for IDPs [8].

In summary, we have shown that the rapid but marginally stable conformational fluctuations that are particularly relevant for IDPs can be observed and characterized using force spectroscopy. From the kinetics of these structural fluctuations, the energy landscape profile was quantified, revealing the flat but rugged landscape expected to be a hallmark of IDPs. Extending this approach to study $\alpha$-synuclein under conditions in which it is more prone to aggregate, as well as to study other aggregation-prone IDPs, should provide quantitative insight into the features of the energy landscape that relate to the aggregation process.

This work was supported by Canadian Institutes of Health Research Grant No. NHG 91374, Alberta Innovates (AI) Technology Futures and AI Health Solutions, and the National Institute for Nanotechnology. A. S. acknowledges support from AI Technology Futures. A. S. and K. N. contributed equally to this work.

[1] A. K. Dunker, Z. Obradovic, P. Romero, E. C. Garner, and C. J. Brown, Genome Inf. Ser. **11**, 161 (2000).
[2] P. Tompa, Trends Biochem. Sci. **37**, 509 (2012).
[3] H. J. Dyson, Q. Rev. Biophys. **44**, 467 (2011).
[4] A. K. Dunker *et al.*, J. Mol. Graphics Modell. **19**, 26 (2001).
[5] B. A. Shoemaker, J. J. Portman, and P. G. Wolynes, Proc. Natl. Acad. Sci. U.S.A. **97**, 8868 (2000).
[6] H. J. Dyson and P. E. Wright, Nat. Rev. Mol. Cell Biol. **6**, 197 (2005).
[7] V. N. Uversky, C. J. Oldfield, and A. K. Dunker, Annu. Rev. Biophys. **37**, 215 (2008).
[8] V. N. Uversky, BBA Proteins Proteo. **1834**, 932 (2013).
[9] A. J. Trexler and E. Rhoades, Biochemistry **48**, 2304 (2009).
[10] A. C. Ferreon, Y. Gambin, E. A. Lemke, and A. A. Deniz, Proc. Natl. Acad. Sci. U.S.A. **106**, 5645 (2009).
[11] G. Veldhuis, I. Segers-Nolten, E. Ferlemann, and V. Subramaniam, Chem. Bio. Chem. **10**, 436 (2009).
[12] A. J. Trexler and E. Rhoades, Biophys. J. **99**, 3048 (2010).
[13] P. H. Weinreb, W. Zhen, A. W. Poon, K. A. Conway, and P. T. Lansbury, Biochemistry **35**, 13709 (1996).
[14] W. S. Davidson, A. Jonas, D. F. Clayton, and J. M. George, J. Biol. Chem. **273**, 9443 (1998).
[15] T. Bartels, J. G. Choi, and D. J. Selkoe, Nature (London) **477**, 107 (2011).
[16] M. Vilar, H.-T. Chou, T. Lührs, S. K. Maji, D. Riek-Loher, R. Verel, G. Manning, H. Stahlberg, and R. Riek, Proc. Natl. Acad. Sci. U.S.A. **105**, 8637 (2008).
[17] M. Sandal, F. Valle, I. Tessari, S. Mammi, E. Bergantino, F. Musiani, M. Brucale, L. Bubacco, and B. Samorì, PLoS Biol. **6**, e6 (2008).
[18] R. Hervas *et al.*, PLoS Biol. **10**, e1001335 (2012).
[19] J. Yu, S. Malkova, and Y. L. Lyubchenko, J. Mol. Biol. **384**, 992 (2008).
[20] W. J. Greenleaf, M. T. Woodside, and S. M. Block, Annu. Rev. Biophys. **36**, 171 (2007).
[21] K. Neupane, A. Solanki, I. Sosova, M. Belov, and M. T. Woodside, PLoS One **9**, e86495 (2014).
[22] H. Yu, X. Liu, K. Neupane, A. N. Gupta, A. M. Brigley, A. Solanki, S. Iveta, and M. T. Woodside, Proc. Natl. Acad. Sci. U.S.A. **109**, 5283 (2012).
[23] H. Yu, A. N. Gupta, X. Liu, K. Neupane, A. M. Brigley, I. Sosova, and M. T. Woodside, Proc. Natl. Acad. Sci. U.S.A. **109**, 14452 (2012).
[24] See Supplemental Material at http://link.aps.org/supplemental/10.1103/PhysRevLett.112.158103 for details on the materials and methods, including Refs. [25–30].
[25] C. Cecconi, E. Shank, F. Dahlquist, S. Marqusee, and C. Bustamante, Eur. Biophys. J. **37**, 729 (2008).
[26] D. B. Ritchie, D. A. N. Foster, and M. T. Woodside, Proc. Natl. Acad. Sci. U.S.A. **109**, 16167 (2012).
[27] M. D. Wang, H. Yin, R. Landick, J. Gelles, and S. M. Block, Biophys. J. **72**, 1335 (1997).
[28] J. Kim, C.-Z. Zhang, X. Zhang, and T. A. Springer, Nature (London) **466**, 992 (2010).
[29] L. Pauling and R. B. Corey, Proc. Natl. Acad. Sci. U.S.A. **37**, 251 (1951).
[30] I. Tinoco, Jr. and C. Bustamante, Biophys. Chem. **101–102**, 513 (2002).
[31] M. Rief, M. Gautel, F. Oesterhelt, J. M. Fernandez, and H. E. Gaub, Science **276**, 1109 (1997).
[32] J. Stigler, F. Ziegler, A. Gieseke, J. C. M. Gebhardt, and M. Rief, Science **334**, 512 (2011).
[33] M. Schlierf, F. Berkemeier, and M. Rief, Biophys. J. **93**, 3989 (2007).
[34] G. Žoldák, J. Stigler, B. Pelz, H. Li, and M. Rief, Proc. Natl. Acad. Sci. U.S.A. **110**, 18156 (2013).
[35] R. V. Dalal, M. H. Larson, K. C. Neuman, J. Gelles, R. Landick, and S. M. Block, Mol. Cell **23**, 231 (2006).
[36] M. T. Woodside, W. M. Behnke-Parks, K. Larizadeh, K. Travers, D. Herschlag, and S. M. Block, Proc. Natl. Acad. Sci. U.S.A. **103**, 6190 (2006).

[37] K. Neupane, D. B. Ritchie, H. Yu, D. A. N. Foster, F. Wang, and M. T. Woodside, Phys. Rev. Lett. **109**, 068102 (2012).
[38] O. K. Dudko, G. Hummer, and A. Szabo, Proc. Natl. Acad. Sci. U.S.A. **105**, 15755 (2008).
[39] M. M. Dedmon, K. Lindorff-Larsen, J. Christodoulou, M. Vendruscolo, and C. M. Dobson, J. Am. Chem. Soc. **127**, 476 (2005).
[40] C. W. Bertoncini, Y.-S. Jung, C. O. Fernandez, W. Hoyer, C. Griesinger, T. M. Jovin, and M. Zweckstetter, Proc. Natl. Acad. Sci. U.S.A. **102**, 1430 (2005).
[41] S. McClendon, C. C. Rospigliosi, and D. Eliezer, Protein Sci. **18**, 1531 (2009).
[42] P. J. Elms, J. D. Chodera, C. Bustamante, and S. Marqusee, Proc. Natl. Acad. Sci. U.S.A. **109**, 3796 (2012).
[43] P. Hanggi, P. Talkner, and M. Borkovec, Rev. Mod. Phys. **62**, 251 (1990).
[44] B. Ahmad, Y. Chen, and L. J. Lapidus, Proc. Natl. Acad. Sci. U.S.A. **109**, 2336 (2012).
[45] V. R. Singh and L. J. Lapidus, J. Phys. Chem. B **112**, 13172 (2008).
[46] N. D. Bouley Ford, D.-W. Shin, H. B. Gray, and J. R. Winkler, J. Phys. Chem. B **117**, 13206 (2013).
[47] D. Nettels, I. V. Gopich, A. Hoffmann, and B. Schuler, Proc. Natl. Acad. Sci. U.S.A. **104**, 2655 (2007).
[48] R. Zwanzig, Proc. Natl. Acad. Sci. U.S.A. **85**, 2029 (1988).
[49] B. G. Wensley, L. G. Kwa, S. L. Shammas, J. M. Rogers, S. Browning, Z. Q. Yang, and J. Clarke, Proc. Natl. Acad. Sci. U.S.A. **109**, 17795 (2012).
[50] J. N. Onuchic and P. G. Wolynes, Curr. Opin. Struct. Biol. **14**, 70 (2004).
[51] K. A. Dill and J. L. MacCallum, Science **338**, 1042 (2012).